Chapter 3

Preparation, characterization, *in-vitro* and *in-vivo* pharmacokinetic evaluation of dimethyl fumarate cocrystal with basic coformer (Nicotinamide)

3 Preparation, characterization, *in-vitro* and *in-vivo* pharmacokinetic evaluation of dimethyl fumarate cocrystal with basic co-former (Nicotinamide)

3.1 Introduction

A cocrystal denotes two or more two molecules that have been combined into the same crystal lattice through intermolecular interactions like hydrogen bonding, p-p stacking, and van der Waals forces with a fixed stoichiometric ratio, creating a special multicomponent supramolecular crystal structure. Cocrystals comprise API and benign molecules or other APIs as coformers [125] via hydrogen bond interaction [126]. As hydrogen bonds rely on hydrogen bond donor and acceptor characteristics of functional groups, coformers are selected cautiously based on the nature of API. It is also essential to establish whether a reaction between an API and a coformer will result in a cocrystal or salt formation. [127]. Salt or cocrystal formation can be predicted from the pKa values of coformer and API being chosen [128]. The supramolecular synthon approach, which utilizes the Cambridge Structural Database (CSD) to effectively prioritize coformers for crystal form screening, is another useful tool for making cocrystals [129]. DMF has four hydrogen bond acceptors measured using Cactvs 3.4.6.11 (PubChem release 2019.06.18), which makes it a potential molecule to undergo cocrystallization. Cocrystals of DMF with gentisic acid and camphoric acid have been reported to show enhanced absorption and bioavailability [130]

Dimethyl fumarate (DMF) is an FDA-approved drug for treating relapsing-remitting multiple sclerosis and psoriasis. It has antioxidant, anti-inflammatory, and immunomodulatory properties, which contribute to its efficacy in diseases [131]. It is available as an oral drug in tablet and capsule forms and in the body, it is hydrolyzed into an active metabolite-monomethylfumarate (MMF). DMF has a physiochemical disadvantage as it sublimates at a relatively low temperature and when processed

conventionally, about 15-20% of DMF is lost from the final formulation and upon storage [70]. This is most likely because of sublimation during production. Sublimation also leads to the loss of DMF during long-term storage from bulk and its formulations as well. DMF owes some serious gastrointestinal (GI) adverse effects anal incontinence, diarrhea, dyspepsia, irritable bowel syndrome, gastritis, erosive gastritis, gastric ulcer and gastroduodenitis [67, 68]. Cocrystal has been used to improve thermodynamic stability [132], and physicochemical properties like solubility and dissolution profile of the drugs [133]. There are many instances of drug-drug cocrystals as well as having beneficial effects together [134].

Nicotinamide has been used extensively to make cocrystals for altering the physicochemical properties of many drugs [135]. Nicotinamide, a coformer possesses a single hydrogen bond donor with two acceptors count as computed by Cactvs 3.4.6.11 (PubChem release 2019.06.18). cytoprotective effect of nicotinamide against indomethacin-induced gastric lesions, not only by virtue of its antioxidant potential but also due to its ability to restore gastric mucus, nitric oxide contents, and attenuation of the enhanced gastric microvascular permeability [136].

Cocrystals can be made from a plethora of methods including liquid-assisted grinding, slurry conversion, supercritical fluid method and solution methods. We have utilized the solvent evaporation method due to its high efficacy and reproducibility of cocrystallization [137]. This technique involves the nucleation and growth of cocrystals from a solution containing coformers and the API with loss of solvent via evaporation of the solvent. In the solvent evaporation method, the size of the crystals can be controlled by modulating the rate of evaporation of the solvent, providing it an edge over other methods of cocrystallization [72].

DMF is a prodrug with monomethylfumarate (MMF) as its primary metabolite [138] but many studies have shown DMF to exert more cytoprotective effect than MMF [139]. Once Absorbed DMF/MMF rapidly penetrates blood cells mainly peripheral blood mononuclear cells (PBMC) and covalently binds to GSH and other molecules [111]. PBMC analysis is one of the important parameters to evaluate the pharmacological actions of DMF and LPS-induced inflammation in PBMC has been utilized in this work to evaluate the anti-inflammatory activity of DMF and formulated cocrystal [140]. Moreover, DMF is well known to decrease the synthesis of pro-inflammatory mediators like TNF-α, IL-1β, ROS, and IL-6 in activated microglia and astrocytes and in LPS-activated PBMCs [141] so we have evaluated the effect of DMF and the cocrystals on change in intracellular ROS, TNF-α and IL-6 activity in LPS induced PBMC.

The cocrystallization approach is a reliable method to modulate the physicochemical properties of drug molecules. Sublimation-mediated loss of DMF and its gastric-related adverse effects have motivated us to formulate its cocrystals using nicotinamide as a coformer. We have characterized our cocrystals using thermal stability indicators such as DSC, TGA and thermal assault. Spectral tools like FTIR and PXRD further support cocrystallization. To evaluate the thermostability of the cocrystals, we have exposed DMF and the formulated cocrystals to an extreme condition of 60°C and 75% RH for 20 days. We have compared DMF and its formulated cocrystals for *in-vitro* cytotoxicity LPS-induced alterations in ROS, IL-6, and TNF-α in PBMC. We have also performed *in-vitro* dissolution and *in-vivo* pharmacokinetic profiling of DMF with that of the cocrystals. The gastroprotective effect of the cocrystal has been evaluated against the acute ulcer model and acetic acid-induced ulcer healing model.

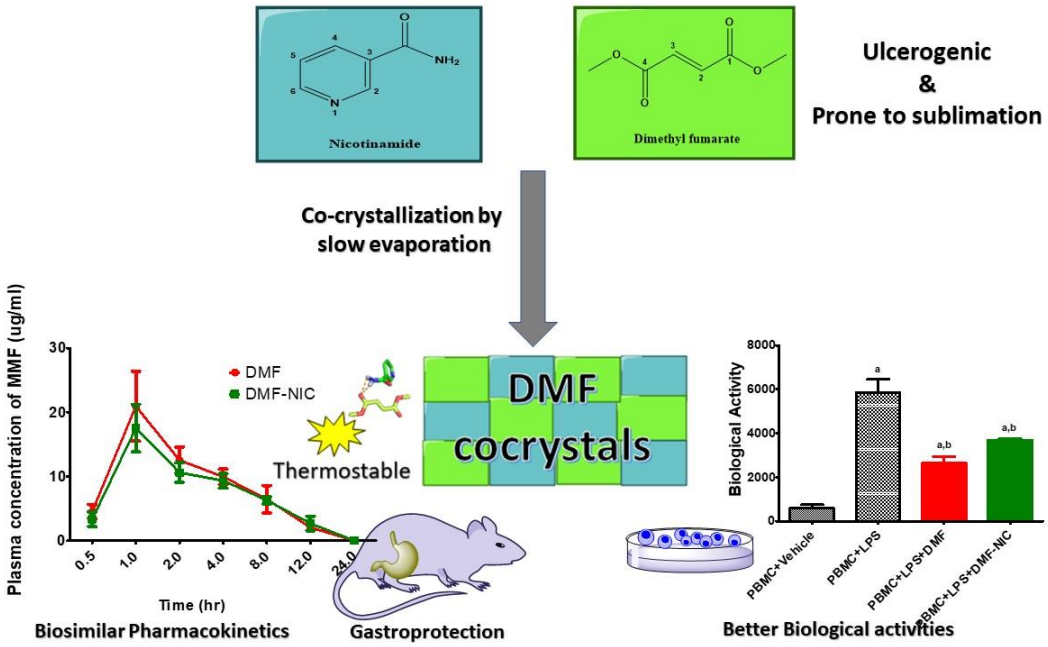

Figure 3-1 The proposed hypothesis.

3.2 Materials and Methods

3.2.1 *In-silico* work

3.2.2 Molecular docking

The structures of nicotinamide and dimethyl fumarate were sketched with the help of Chemdraw 15. Further, they were converted into three-dimensional structures through energy minimization using MMFF94s force field. These mol2 files were converted to pdbqt using Autodock tools 1.5.6. Autogrid-4.0 was used to calculate grid maps of interaction energies among the various types of atoms present (A, C, HD, NA, N, OA, S). The grid box size was set to 40 × 40 × 40 with a grid spacing of 0.375 Å. The grid centered on coordinates (x, y, and z) 0.423, 0.316 and 0.0. The docking was performed by Autodock-4.2.6 using Lamarckian Genetic Algorithm with 10 runs, 150 population size, 2,500,000 maximum number of energy evaluations and 27,000 maximum number of generations [142, 143]. The docked structure was visualized by using Discovery Studio 2020 [144].

3.2.3 Molecular dynamics

The obtained poses of ligands were parameterized through *antechamber* toolkit using general AMBER force field (GAFF2) and the Austin model with bond and charge correction (AM-BCC1) atomic partial charges. The topologies and coordinates for the complex of DMF and NIC were build using *tleap* module of AMBER 20. It hydrated with TIP3P water molecules in a cubic box with a cut-off distance of 12 Å and neutralized by adding Na+ and Cl- ions. The systems were subjected to energy minimization, heating, density equilibration and equilibration under periodic boundary conditions [145]. The final 5 ns molecular dynamics (MD) was carried out at 310.15 K as an NPT ensemble. Further, the post-MD processing was carried out using *cpptraj* [146-148].

3.2.4 Experimental Animals

Inbred male adult Sprague-Dawley rats weighing between 180 g and 220 g (8 to 10 weeks old) male rats were procured from Central Animal House; Institute of Medical Science (IMS-BHU). The experiments were performed by adopting guidelines (NIH publication number 85-23, revised 2015) and approved by the Institutional Animal Ethical Committee, Banaras Hindu University (BHU; Dean/2019/CAEC/1649). Animals were acclimatized in the experimental lab before using them for experiments for a period of one week of acclimatization under standard laboratory conditions (22 ± 2 °C, 12 h light/dark cycle, and relative humidity of 50 ± 5%).

3.2.5 Materials

DMF was obtained from Disto Pharmaceuticals (Hyderabad, India) as a gift sample, nicotinamide, and sodium chloride were purchased from Merck, MTT was obtained from SRL chemicals, Hisep was obtained from Himedia (India), LPS (E. coli, L3129), MMF, dichlorofluorescin diacetate, trypan blue and antibiotics were obtained from Sigma

Aldrich, RPMI-1640 and FBS were obtained from Lonza, TNF-α and IL-6 ELISA kits were purchased from Krishgen Biosystems (Mumbai, India). Ultrapure water was prepared using a Milli-Q Ultrapure purification system (Millipore, USA). Countess™ Cell Counting Chamber Slides were purchased from Thermo Fisher (USA). All other chemicals and reagents of high-performance liquid chromatography (HPLC) and analytical grade were procured from the local suppliers.

3.2.6 Method of Preparation

The cocrystal was formulated by the solvent evaporation method [149]. It is a commonly used method for the preparation of cocrystals. This technique is based on the solubility profile of the API and the coformers. The method requires the drug substance and the coformer to get dissolved in a common solvent which is allowed to evaporate slowly over a period of time. The technique works on the principle of the formulation of hydrogen bonds in a favorable drug substance and a complementary coformer [72].

3.2.7 Formulation

For making DMF-nicotinamide cocrystal (DMF-NIC), DMF and nicotinamide were taken in 1:1 molar ratio and dissolved separately in an excess of ethanol. Both were mixed to get a clear homogenous solution. The solution was passed through a 0.22 µm membrane filter to avoid any undissolved particles. It was kept in a glass container fully covered with aluminum foil with small holes over it to facilitate solvent evaporation. It was kept undisturbed in an incubator set at 40°C for slow solvent evaporation in order to get fine cocrystals. The evaporation rate controls the process of crystallization, more time is provided for evaporation, the larger the crystals are obtained. The resulting product was dried in an oven at 80 °C overnight to remove residual solvent and gently ground to a fine powder for further analysis.

3.3 Characterization of cocrystals

3.3.1 Attenuated total reflectance FTIR (ATR- FTIR) spectroscopy

FTIR spectral region was set from 400 to 4000 cm^{-1} obtained using a Shimadzu IR-Prestige-21 FTIR spectrometer coupled with a horizontal Golden Gate MKII single-reflection ATR system (Specac, Kent, UK) equipped with ZnSe lenses after appropriate background subtraction. All the spectral data were collected at ambient temperature. Data were collected and analyzed by the built-in software.

3.3.2 Powder X-ray Diffraction (PXRD)

PXRD was conducted by a MiniFlex II benchtop X-ray diffractometer at 30 kV and 15 mA with a Ni-filtered Cu KR radiation source (λ) 1.54 Å) (Rigaku, The Woodlands, TX, U.S.A.). The samples were scanned from 5° to 30° (2θ) at a scanning rate of 0.5°C per min. The diffractograms were processed using Origin Pro.

3.3.3 Thermal stability evaluation of cocrystals

Melting point is one of the essential physical properties of solids, which is used to determine the purity of the product. A high melting point demonstrates the thermodynamic stability of the new materials i.e. thermal stability of an API can be increased by selecting the coformer with the higher melting point [150]. The most commonly used techniques for the determination of melting point and thermal stability analysis are thermal gravimetric analysis (TGA) and differential scanning calorimetry (DSC) [151]. The melting point of pharmaceutical cocrystals can be tailored by judicious selection of the coformers which could provide thermal stability to the complimentary API [152].

3.3.4 Differential Scanning Calorimetry (DSC)

DSC was conducted by use of a DSC-60 Plus Shimadzu Differential scanning calorimeter. Accurately weighed samples (4-7 mg) were placed in hermetically sealed aluminium pans and scanned from 25 to 250°C at 10 °C/min under a nitrogen purge. The DSC calibration was done using the single-point method with the extrapolated onset of the melting point of a 0.275 mg sample of indium.

3.3.5 Thermogravimetric Analysis (TGA)

The decomposition temperature for each substance was determined using Shimadzu. Corporation TGA-50 Thermo-gravimetric analyzer. Approximately (4-7 mg) amount of sample was heated from 25 to 250 °C at a 10 °C/min rate. A purge of dry nitrogen (flow rate sample, 60 mL/min; flow rate balance, 40 mL/min) was maintained through the sample chamber during all the experiments to keep an inert environment and to avoid any oxidation of samples.

3.3.6 Evaluation of Sublimation behavior

The sublimation behavior of DMF and the cocrystals was evaluated by following the method of physical stability with some modifications [153]. A known amount of DMF and DMF-NIC cocrystal and their physical mixtures was prepared by gentle trituration of the DMF and the coformer in the same ratios which have been taken for cocrystal in a glass vial. The mouth of the glass vials was covered with perforated aluminum foil. These glass vials were maintained in an incubator at 60 °C,75% RH for a period of 20 days. As approximately 80% of DMF sublimed by 20^{th} day, it was kept in this condition for not more than 20 days. Relative humidity was maintained using a saturated solution of sodium chloride kept in a beaker in the same incubator [154]. % DMF sublimed was analyzed after 10 and 20 days respectively from the day it was kept in the incubator.

3.3.7 Dissolution

Dissolution was carried out following the method as per FDA (www.accessdata.fda.gov/scripts/cder/dissolution) 100 mg each of DMF and various cocrystals were filled into empty capsule shells and taken into 500 mL phosphate buffer (pH 6.8) at the beginning of the dissolution experiments. The mixtures in the dissolution tester were stirred at 37 °C and 100 rpm. At each time interval, 5 mL of the solution was withdrawn from the instrument and replaced by an equal volume of buffer to maintain the sink condition in the experiment. The solution was filtered by a 0.22 μm nylon filter before measuring DMF concentration and were analyzed by HPLC.

3.3.8 HPLC analysis

DMF quantification was performed by HPLC using Agilent technologies HPLC, Infinity 1260 II equipped with a degasser, a quaternary pump, and an autosampler. 20A3), The system includes a diode array detector and a computer running Agilent openLAB CDS control panel help software for data acquisition and processing. Chromatographic separation was performed at 25±1 °C, by using a C8 column (4.6 X 250 mm, 5μm) preceded by a guard column of the same packing material. The mobile phase used consisted of acetonitrile and water (80:20). The flow rate was set at 1.0 mL/min and the total sample acquisition time was 10 min. Based on previous studies, the UV detector was set at 220 nm and the injection volume was set at 10 μl. For MMF quantification, the solvent system was methanol: potassium phosphate buffer supplemented with 5 mM tetrabutylammonium dihydrogen phosphate 20 : 80 (v/v) with a detector set at 215 nm [155].

3.4 *In vitro* evaluation of biological activity of cocrystals

3.4.1 Isolation of peripheral blood mononuclear cells (PBMCs)

To measure the effect of DMF and Its cocrystals on PBMC, blood was obtained from a Sprague−Dawley rat through the terminal method (cardiac puncture) and taken into EDTA vacutainer tubes. It was diluted with an equal volume of PBS. Mononuclear cells were separated from peripheral blood samples according to the method described with modification [140, 156]. Briefly, 3 ml of blood mixture was gently layered over 2 ml of Hisep (Ficoll) solution and centrifuged at 1000 g for 25 min. The white band of mononuclear cells was collected and washed thrice with RPMI 1640 culture medium by centrifugation at 1000 g for 5 min. PBMCs were resuspended in complete RPMI 1640 culture medium (RPMI 1640 medium containing 25 mM HEPES, 2 mM L-glutamine, 10% heat-inactivated fetal calf serum, penicillin (100 U/ml) and streptomycin (100 μg/ml)) and adjusted to 2×10^6 cells/ml.

3.4.2 PBMC counting via Trypan blue exclusion (TBE) assay

Cell count was done using the trypan blue dye exclusion technique with the help of Countess™ II automated cell counter using the Trypan Blue exclusion (TBE) method [157]. After isolating the PBMC, 10 μl aliquots of the sample were mixed with 10 μl of Trypan blue (0.4%) (Invitrogen, Italy). It was put into a Countess™ cell counting chamber slides and the count was made by a Countess® automated cell counter (Invitrogen, Italy).

3.4.3 Cytotoxicity assay

MTT assay was performed to evaluate the cytotoxicity of cocrystals when compared with the pure DMF following [158] with slight modifications. MTT dye via reductive cleavage of its tetrazolium ring is converted to purple water-insoluble formazan in the presence of

mitochondrial succinate dehydrogenase in living cells. Thus, the assay signifies the ability of metabolically active cells to reduce MTT to formazan. In other words, the amount of formazan produced serves as a direct indicator of the number of viable cells in the sample. 100 µl of PBMC aliquot containing (approximately 2,00,000 cells) was taken in RPMI-1640 containing 20% FBS in a microculture well. 20 µg/ml and 10 µg/ml of cocrystals and DMF were added into the microculture well. Blank and vehicle control groups were taken. The culture plate was incubated for 12 hours at 37°C in 5% CO_2 condition in the incubator chamber. 10 µl of MTT (5 mg/ml) was added into the microculture wells and again kept for 2 hours at 37°C and 5% CO_2 condition in the incubator. 100 µl of DMSO was added to it and kept again for 2 hours. Absorbance was taken at 570 nm.

3.4.4 Cytokine analysis

Evaluation of cocrystals on LPS-induced PBMC following [159] with slight modifications. PBMC ($2X10^6$ cells/ml) was separated from each rat and 100 µl of PBMC aliquot containing (approximately 2,00,000 cells) was incubated with and without LPS (10 µg/ml) in 100 µl RPMI containing 20% FCS for 24 hr in a humidified atmosphere of 5% CO_2 at 37 ºC. Later it was washed twice with PBS and incubated with DMF and various cocrystals containing an equivalent of 10 µg/ml DMF for 12 hours. It was washed twice again with PBS. Further, it was incubated for 2 hr with RPMI Containing 20% FCS. It was centrifuged at 1500xg for 5 min to obtain a clear supernatant. The supernatant was cryopreserved for further Cytokine's activity. IL-6 and TNF-α levels in the supernatant were determined using commercial enzyme-linked immunosorbent assay (ELISA) kits.

3.4.5 Measurement of intracellular ROS (iROS)

Intracellular ROS was detected using DCFH-DA, which crosses cell membranes and gets hydrolyzed into nonfluorescent DCFH by intracellular esterases. However, DCFH is oxidized to a highly fluorescent dichlorofluorescein (DCF), in the presence of ROS, which is readily detectable by fluorescence-based instruments like FACS or spectrofluorometer. Intracellular ROS were measured in the PBMC treated with LPS and further DMF and its respective cocrystals were evaluated against LPS using the following method [160]. PBMC were counted for total viable cells by trypan blue exclusion assay with the help of Countess™ II automated cell counter. In order to generate cellular reactive oxygen species in the PBMC, 100 µl aliquot of PBMC containing (approximately 2,00,000 cells) was incubated with LPS (10 µg/ml) in 100 ul RPMI containing 20% FCS for 24 h in a humidified atmosphere of 5% CO2 at 37 ºC by the method given by Alaimo [161]. Later it was washed twice with PBS and incubated with 10 µg/ml DMF and various cocrystals containing equivalent 10 µg/ml DMF for 12 hours. It was washed twice again with PBS. iROS were labelled by incubating cells in 100 µl of 20 mM dichlorofluorescein diacetate (DCFH-DA) for 45 min at 37 °C temp in the dark. After incubation, fluorescence intensity was monitored by using a fluorescence spectrometer (λex: 490 nm; λem: 515 nm).

3.4.6 Pharmacokinetic study

Pharmacokinetic data of DMF and its cocrystals were evaluated in healthy male Sprague−Dawley rats weighing 150−200 g (8 to 10 weeks old), following the method [162]. Animals were divided into four groups including 3 animals in each group. Animals were kept fasting overnight before the experiment but water was given *ad libitum*. The animals were given an oral dose of 100 mg/kg of DMF and its cocrystals containing the

same amount of DMF. Blood samples (0.25ml) were isolated via retro-orbital under ether anesthesia in the heparin-treated tube at 0.5 h, 1 h, 2 h, 4 h, 8 h, 12 h and 24 h. Plasma was isolated from blood samples by centrifuging the blood samples at 7000 rpm for 5 min at 4° C. The isolated plasma containing the drug (DMF) was extracted by precipitating it with an equal volume of acetonitrile. It was vortexed for a minute and later centrifuged at 13000 rpm for 15 min. The clear supernatant was isolated and filtered 0.22 µm used for further analysis using HPLC.

3.4.7 Acute ulcer model of rat

DMF is known to cause GIT irritation, anal incontinence, diarrhea, dyspepsia, irritable bowel syndrome, and peptic ulcer [163, 164]. We have developed an acute gastric ulcer model with DMF taking DMF at a higher dose (400 mg/kg) which has been shown to cause gastric ulceration.

Animals were divided into three groups containing five animals in each group namely Vehicle control, DMF group and DMF-NIC group respectively. Animals were fasted for 16 hr by placing them in a cage with a perforated base in order to avoid coprophagy. Water was given *ad libitum.* Acute gastric ulcer was induced by dosing the animals with DMF (400 mg/kg) dispersed in 0.5% CMC and DMF-NIC containing 400 mg/kg of DMF dispersed in 0.5% CMC, The vehicle group was provided with 0.5% CMC only. Dosing was done by intragastric route using a long smooth gastric tube in order to avoid gastritis of the oral and esophageal mucosal layer.

3.4.8 Acetic acid-induced chronic gastric ulcers in rats

The acetic acid model of gastric ulcers is an easy and common method that has some resemblance to an acute chronic gastric ulcer in humans. Chronic gastric ulcers were

induced in rats by the method of [165] with slight modifications. Sprague-Dawley rats were randomly assigned into five groups consisting of five animals in each group. The animals were deprived of food for 24 hours but were allowed free access to water before gastric ulcer induction. They were kept in a net-based perforated cage to avoid coprophagy. Briefly, animals were anesthetized with ketamine, (60 mg/kg) and xylazine (5 mg/kg) *intraperitoneal* administration. When anaesthetization is confirmed a cut of an approximate 2 cm opening was made from the middle of the xiphoid process along the middle line of the abdomen. The stomach is traced and it is gently pulled out without disturbing the other vitals. The antrum wall of the stomach was identified and it was cleaned with a smooth cotton swab. Meanwhile, make a disc of filter paper about 5 mm in diameter and specified thickness (measurement kept constant for the experiment) dipped with the proper amount of glacial acetic acid (99.5%). It was applied for 30 s × 2 times (one filter paper per time) to the serous layer of the antrum of the stomach. Immediately the surface containing acetic acid was wiped away and it was washed with PBS buffer. The rats were taken care till they recovered. These rats were fasted for one day. For the control group rats were treated with the filter paper soaked in PBS only. After 48 hours of the ulcer induction, groups of animals were treated with water to the vehicle group, DMF to the acetic acid+DMF group, cimetidine as the standard treatment group and DMF-NIC cocrystal to the test group once daily for 7 days [166].

3.4.9 Evaluation of gross lesions on the gastric mucosa

The total ulcer area was measured using the National Institute of Health (NIH) image-J software. The ulcer index and the rate of protection of ulceration were calculated by the following formula: Ulcer index was calculated by ulcerated pixel number/total gastric pixel amount X 100 [167].

3.4.10 Determination of related biochemical indexes in gastric tissues

The stomach tissues were weighed, minced with sharp blades, and homogenized with cold PBS buffer, pH 7.2 (w/v,1: 9), and the obtained homogenate was divided into two parts. One of the portions was centrifuged for 10 min at 2500 rpm to obtain the supernatant for the determination of MDA activity and total nitrite level. The total nitrite level was estimated by Griess reagent in which nitrite is assayed in the sample as a reduction product of nitrate into nitrite [168]. The other portion was centrifuged for 10 min at 5000 rpm to determine the level of inflammatory cytokines (TNF-α and IL-6) using specific ELISA kits following the manufacturer's instructions.

3.4.11 Statistical analysis

All values are expressed as the mean ± standard error mean (SEM). Two-way ANOVA followed by Bonferroni post-hoc test was performed to compare % sublimation at day 10 with day 20 and also to compare % cumulative dissolution rate at different time points for DMF and its cocrystals. One-way ANOVA followed by post-hoc student's Newman–Keuls test was performed for the analysis of all other biochemical parameters using Graph Pad Prism version 5 (San Diego, CA). Groups with $p < 0.05$ were considered significantly different. Various spectra were overlayed using Origin 2018. Pharmacokinetic data was analyzed using Kinetika 5.0 software.

3.5 Results

3.5.1 Molecular docking

The docking was employed for the identification of the preferable poses of the interacting coformers, i.e., DMF and NIC in the obtained cocrystal. A Lamarckian genetic algorithm was employed for the generation of the various poses, which were further evaluated through the semiempirical free energy force field-based scoring function of the

AutoDock-4.2.6. It was observed that the docking pose displayed a hydrogen bond between the hydrogen of the amino group of NIC and one of the oxygens, which contributed to the ester bond, of the DMF. Further, the length of the hydrogen bond was found to be 1.89 Å, with a bond energy of -7.523 Kcal/mol, indicating the strength of the bond. It was also observed that both terminal methyl groups of DMF displayed π- alkyl interaction with the phenyl ring of the NIC (**Figure 3-2**).

3.5.2 Molecular dynamics

The MD study was carried out to assess the stability of the interactions between the coformer units with the help of Amber20. A positional restrain force of 10000 Kcal/mol was applied to mimic the interstitial force experienced by the unit cell of a crystal [170]. A 5 ns NPT MD simulation confirmed the stable interaction of DMF and NIC moieties. Root mean square deviation (RMSD) is the indicator of the mean positional deviation of a group of atoms compared to a given frame. The RMSD value of the cocrystal unit was found to be stable, except for the initial 1 ns of the run. The mean RMSD was found to be 0.682 ± 0.196 Å. Further, the mean RMSD for 1 – 5 ns was found 0.748 ± 0.087 Å. The lower value of the standard deviation across this time period indicated stable interactions. The fluctuation about a single atom for the complete simulation time could be measured through root mean square fluctuation (RMSF). The RMSF of all the atoms of both molecules were below 1 Å, which is quite low. Further, the nitrogen atom, a hydrogen donor, in the eighth position of NIC and the oxygen, a hydrogen acceptor, in the seventh position of DMF displayed a lower atomic fluctuation than others. This indicated the formation of a stable hydrogen bond between both molecules. The hydrogen bond analysis indicated the presence of hydrogen bonds between the aforementioned atoms for 81 % of the total simulation time (**Figure 3-2**).

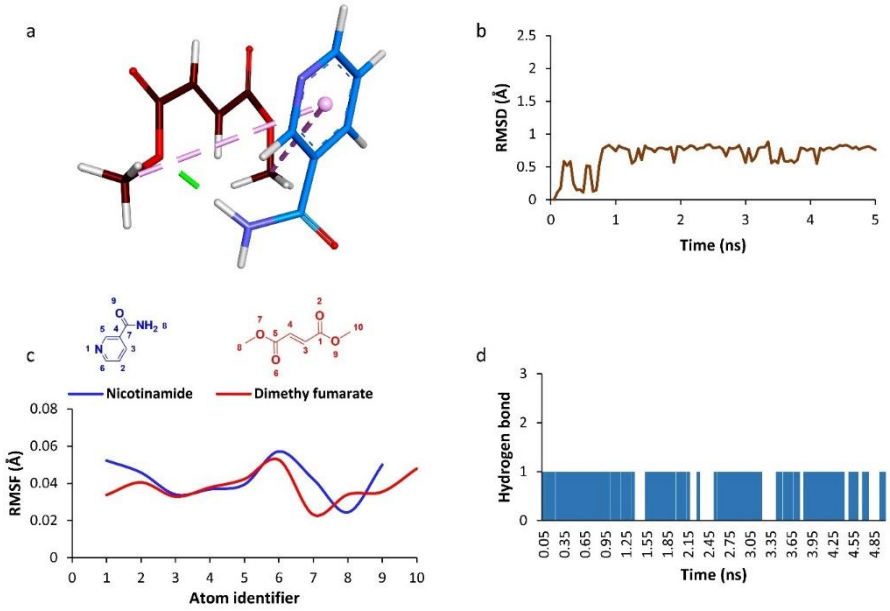

Figure 3-2 (a) 3D interaction between DMF and NIC, (b) RMSD deviation of the system, (c) RMSF deviation of the atoms of DMF and NIC (d) Number of hydrogen bonds between DMF and NIC w.r.t. time.

3.5.3 Characterization of DMF-NIC cocrystal by attenuated total reflectance FTIR (ATR- FTIR)

In **Figure 3-3**, ATR-FTIR spectrum, we have found prominent vibrational peaks in nicotinamide at 1680 cm-1, splitted 3023 cm^{-1} and 3114 $cm^{-1,}$ but redshift was found in the cocrystal leading to peaks at 1685 cm^{-1}, 3004 cm^{-1}, 3068 cm^{-1} respectively. Nicotinamide is a common coformer used for crystallization, similar cocrystal has been obtained by [171].

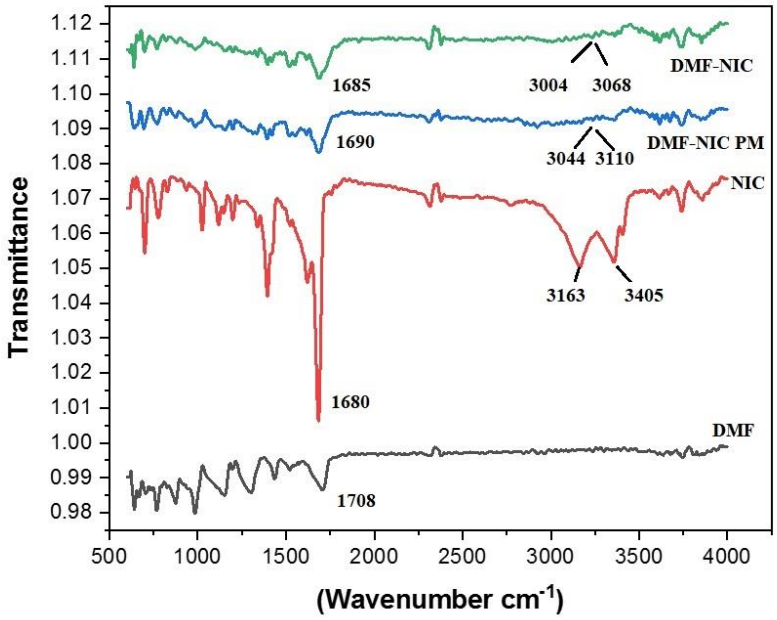

Figure 3-3 IR spectra of DMF and NIC, DMF-NIC Physical mixture, and DMF-NIC cocrystal.

3.5.4 Characterization of DMF-NIC cocrystal by TGA

For DMF-NIC Cocrystal, as shown in **Figure 3-4**, T_{onset} was found to be around 162°C with a single-stage thermogram whereas for pure nicotinamide T_{onset} was found to be 208°C. The cocrystal had provided sufficient chemical and thermal stability to DMF as there was a 2.37% weight loss when it reached T_{onset}.

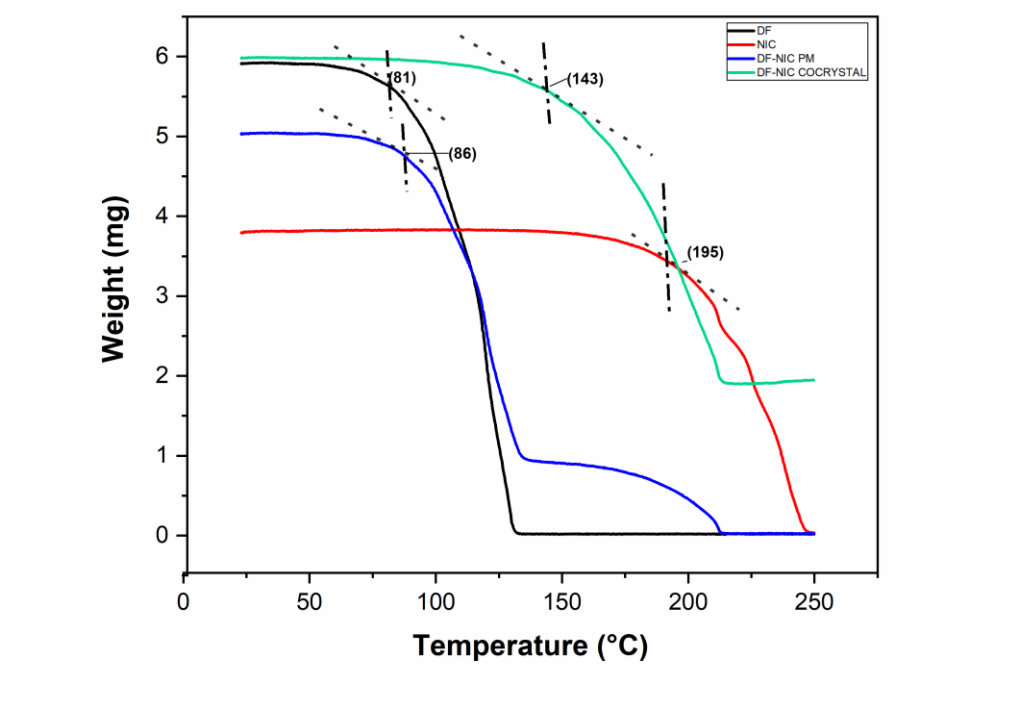

Figure 3-4 TGA thermogram of DMF and NIC, DMF-NIC Physical mixture, and DMF-NIC cocrystal

3.5.5 Characterization of DMF-NIC cocrystal by DSC

In the case of DMF-NIC cocrystal, as shown in **Figure 3-5**, a single sharp peak was obtained at 116 °C but its physical mixture gave endothermic peaks at 103 °C and an elongated broad peak with a sharp emergent peak at 129 °C showing DMF and Nicotinamide. But the extension of the peak thus appeared in cocrystal shows the interaction between them due to the new bond, indicating the formation of cocrystals as for pure nicotinamide, an endothermic peak appeared at 130.0 °C. Many scientists have prepared cocrystals using nicotinamide, and they have obtained a single endothermic peak [153, 172].

The results showed that the melting point of nicotinamide (129 °C) with a higher melting point than DMF gave cocrystal with a high melting point of DMF-NIC cocrystal, 116 °C. The coformer has provided thermal stability to DMF. Similar results were also observed

in one of the studies in which the melting points of cocrystals were proportional to that of the coformers [173].

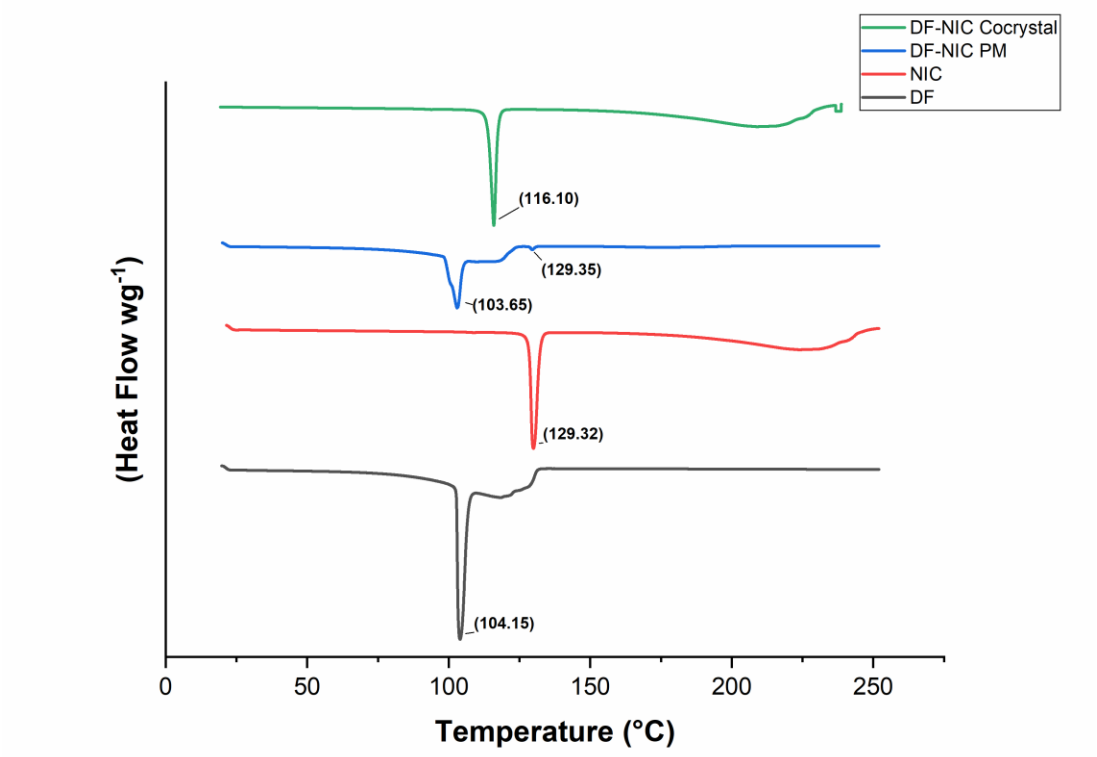

Figure 3-5 TGA thermogram of DMF, Nicotinamide their physical mixture and cocrystal respectively

3.5.6 Characterization of DMF-NIC cocrystal using PXRD

In DMF-NIC cocrystal, as shown in **Figure 3-6**, new peaks appeared at 2θ 13.2°, 16.8°and 29.3° peak heights were altered 2θ at 18.8°, 20.5°, 23. 5°, 28.4° and 29.5° when compared to their physical mixtures.

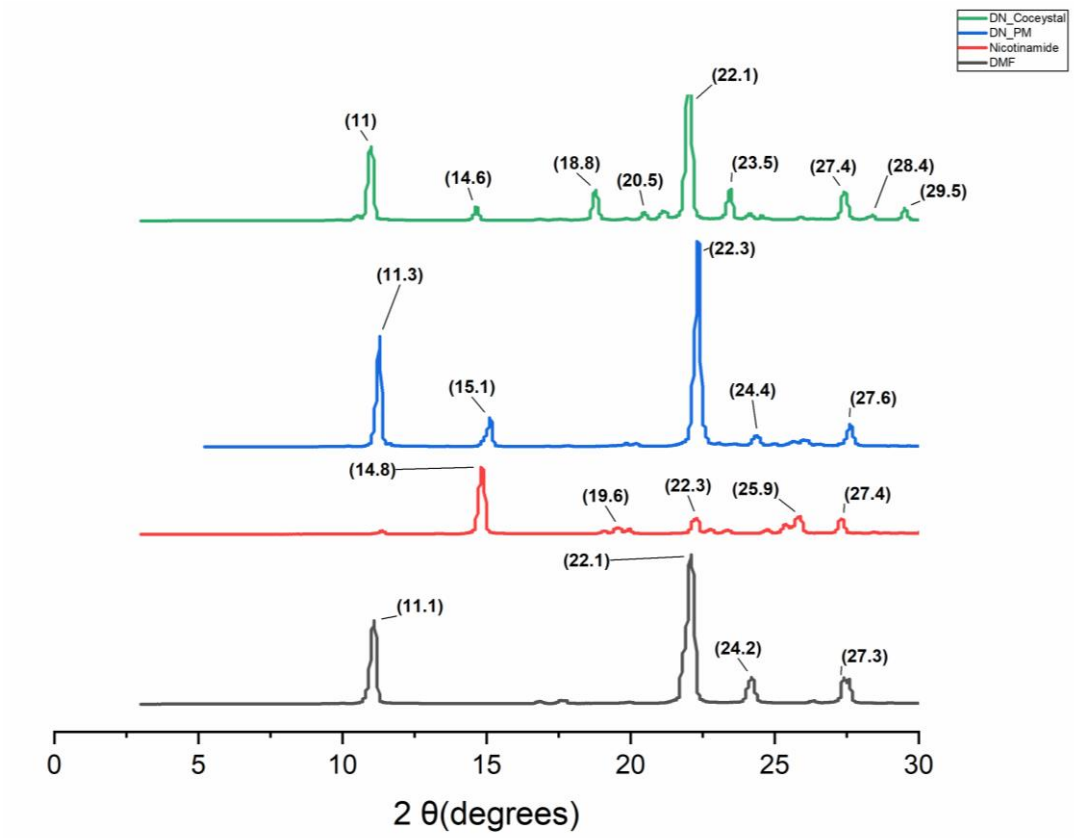

Figure 3-6 PXRD pattern of DMF-Nicotinamide cocrystal.

3.5.7 Effect of cocrystallization on sublimation behaviour of DMF

We kept DMF, their physical mixture and DMF-NIC cocrystal at 60°C, 75% RH maintained in an incubator for a period of 20 days. With reference to the **Figure 3-7** shown below, statistical analysis using one-way ANOVA revealed a significant difference in % sublimed drug [$F(6, 28) = 313.9$, $p < 0.05$]. The post-hoc test revealed that cocrystallization decreased the sublimation of DMF significantly, as we can interpret from the result that the percentage sublimation of DMF was 52.5% as compared to the cocrystals 24 % for DMF-NIC after day-10. We have found that after day-20, DMF had sublimed by 76.5% as compared to the cocrystals which had sublimed by 30.5% for DMF-NIC. Thermal stability has been provided by cocrystalization by interaction via hydrogen bonding [174].

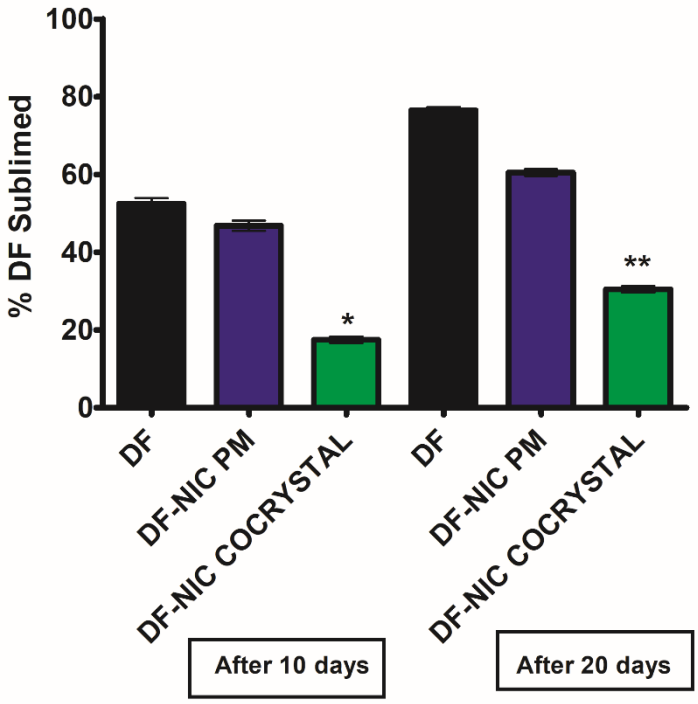

Figure 3-7 Sublimation of DMF, its physical mixture and DMF-NIC cocrystals over 20 days.

*All values are Mean ± SEM (n=3). *p< 0.05 compared to DMF at day-10 and **p< 0.05 compared to DMF at day-20 [one-way ANOVA followed by Newman-keuls Test].*

3.5.8 Effect of cocrystallization on dissolution profile

The dissolution profiles of DMF and DMF-NIC cocrystals were checked to quantify the rate of release of DMF as well as to check whether cocrystal formation has led to any change in the release profile as shown in **Figure 3-8.** Two-way ANOVA revealed significant differences in percent cumulative drug release among groups [F (1, 36) = 23.96, p <0.05], time [F (8, 36) = 388.1, p<0.05] and a significant interaction between groups and arms [F (8, 36) = 1.30, p<0.05]. Statistically, in the case of DMF-NIC cocrystal, we obtained a decrease in drug release at the 120th minute only. It can be explained on the basis that cocrystals alter the solubility and rate of dissolution of API based on its interaction with its coformers including hydrogen bonding, solvent-solute interactions and ionization potential (Maheshwari et al., 2012).

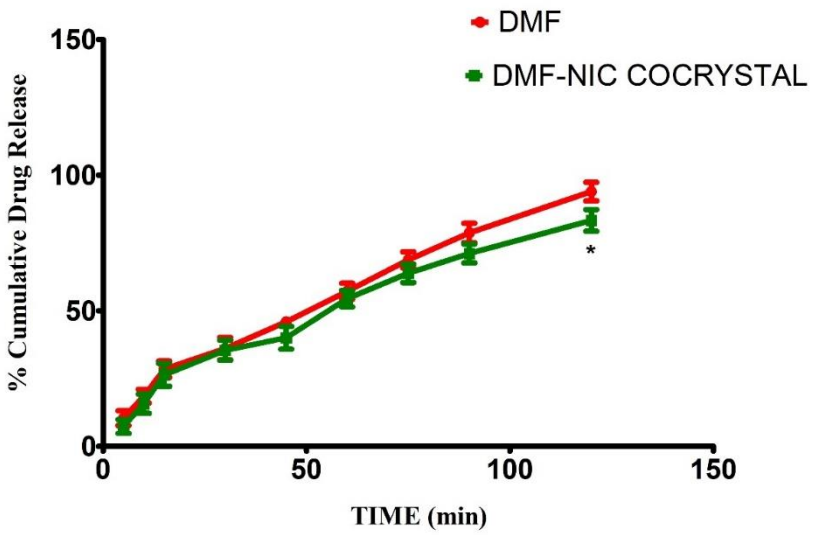

Figure 3-8 Percentage cumulative drug release with time for DMF and its cocrystals.

*All values are expressed as mean ± SEM (n=3) *p< 0.05 compared to DMF [Two-way ANOVA followed by Bonferroni post-hoc test].*

3.5.9 Pharmacokinetics of DMF and DMF-NIC cocrystal

As shown in **Figure 3-9,** two-way ANOVA revealed significant differences in % cumulative drug release among groups [F (1, 12) = 13.79, p <0.05], time [F (6, 12) = 69.06, p<0.05] and a significant interaction between groups and time [F (6, 36) = 2.516, p<0.05]. Post hoc test showed no difference in the plasma concentration of MMF at any time point between the DMF and DMF-NIC cocrystal.

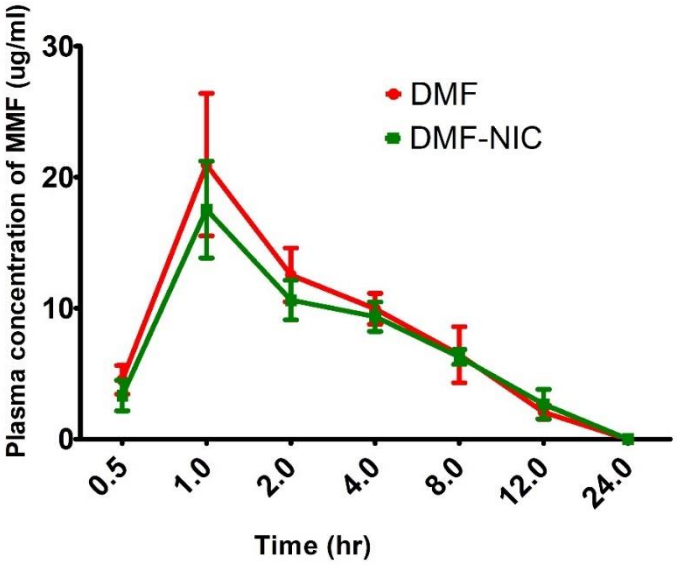

Figure 3-9 Plasma concentration of MMF over 24 hr for DMF and DMF-NIC cocrystal.

All values are expressed as mean ± SEM (n=3). [Two-way ANOVA followed by Bonferroni post-hoc test].

T**able 3 shows,** that statistical analysis using an unpaired t-test revealed no significant difference in the pharmacokinetic parameters (C_{max}, T_{max}, $T_{1/2}$, MRT and AUC) of DMF and DMF-NIC after oral administration.

Table 3 Shows the pharmacokinetic parameters of DMF, DMF- NIC cocrystal.

	DMF	**DMF-NIC**
C_{max} (µg/ml)	20.954 ± 3.145	17.530 ± 2.134
T_{max} (hr)	1.000 ± 0.000	1.000 ± 0.000
$T_{1/2}$ (hr)	3.483 ± 0.294	4.586 ± 0.495
MRT (hr)	5.676 ± 0.346	7.218 ± 0.735
AUC (0-T) (µg*hr/ml)	106.500 ± 1.320	108.900 ± 1.030

All values are expressed as mean ± SEM (n=3). [Student t-test].

3.5.10 Cell viability assay

With reference to the **Figure 3-10** shown below, statistical analysis using one-way ANOVA revealed a significant difference in ulcer area, [F (2, 6) = 2.006, $p<0.05$] The post-hoc test revealed no significant change in the viability of the PBMC cells in DMF and DMF-NIC cocrystal treatment group when compared to the vehicle control group. Thus, DMF and its cocrystals can be considered as non-cytotoxic. Similar results with another cocrystal have been obtained showing non-toxicity of the cocrystal [175].

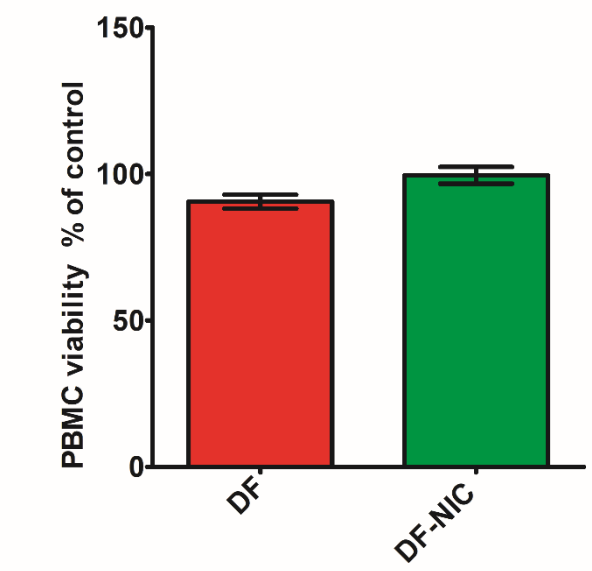

Figure 3-10 Showing PBMC viability of in terms of % control.

All values are Mean ± SEM (n=3) [one-way ANOVA followed by Newman-Keuls Test].

3.5.11 Effect of DMF-NIC cocrystal on oxidative stress

With reference to the **Figure 3-11** shown below, statistical analysis using one-way ANOVA revealed a significant difference in ulcer area, [F (3, 22) = 23.98, $p<0.05$] The post-hoc test revealed significant fluorescence intensity in PBMC+ LPS and PBMC+ LPS+ DMF when compared to the PBMC+vehicle group. Moreover, there was no statistical difference in the fluorescence intensity between the PBMC+vehicle group and

PBMC+ LPS+ DMF+NIC group. DMF is a potent activator of Nrf2 and for its antioxidant activity [176].

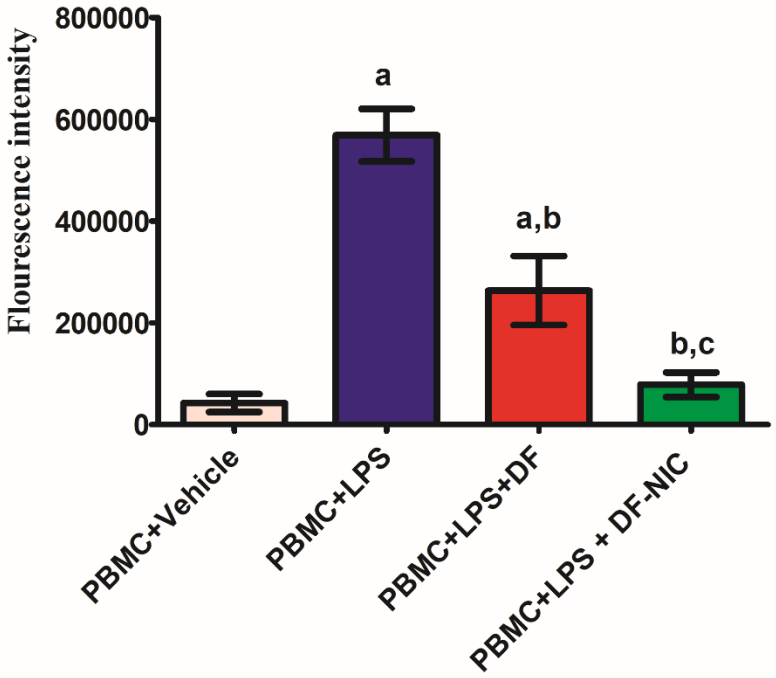

Figure 3-11 ROS activity on treatment with DMF and DMF−NIC cocrystal after LPS induction in PBMC

All values are expressed as mean ± SEM (n=3). [a]p< 0.05 compared to PBMC+vehicle, [b]p< 0.05 compared to PBMC+LPS, [c]p< 0.05 compared to PBMC+LPS+DMF [one-way ANOVA followed by Newman-Keuls Test].

3.5.12 Effect of cocrystals on IL-6 activity

With reference to the **Figure 3-12** shown below, statistical analysis using one-way ANOVA revealed a significant difference in ulcer area, [F (3, 8) = 114.5, p<0.05] The post-hoc test revealed a significant increase in IL-6 concentration in PBMC+ LPS and PBMC+LPS+ DMF and PBMC+ LPS+ DMF+NIC when compared to the PBMC+vehicle group. Moreover, there was no statistical difference in the fluorescence intensity between the PBMC+LPS+DMF group and PBMC+LPS+DMF-NIC group. LPS increases the expression of LPS receptors thereby augmenting the release of IL-6 in

PBMC [156]. DMF and nicotinamide inhibit inflammation by suppressing IL-6 biosynthesis [177, 178] thus, the findings obtained can be justified.

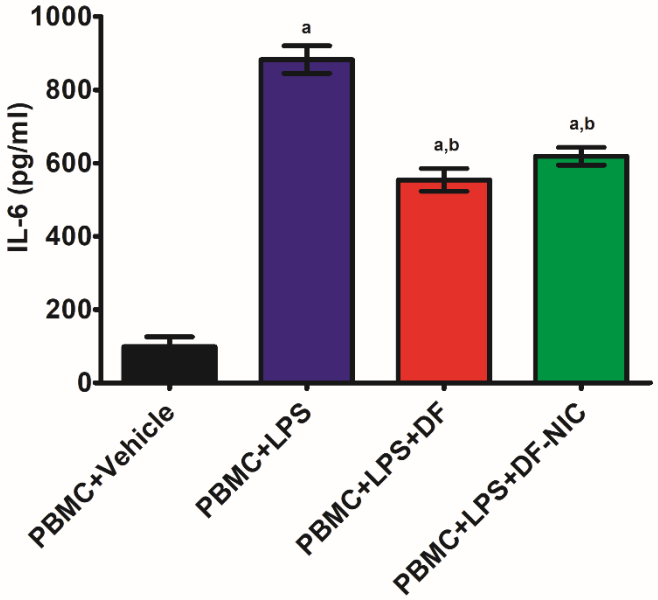

Figure 11 Figure IL-6 activity on treatment with DMF and DMF−NIC after LPS induction in PBMC

All values are expressed as mean ± SEM (n=3). [a]p< 0.05 compared to PBMC+vehicle, [b]p< 0.05 compared to PBMC+LPS [one-way ANOVA followed by Newman-Keuls Test].

3.5.13 Effect of Cocrystals on TNF-α activity

With reference to **Figure 3-13** shown below, statistical analysis using one-way ANOVA revealed a significant difference in TNF-α expression, [F (3, 8) = 40.07, p<0.05] The post-hoc test revealed a significant increase in TNF-α concentration in PBMC+LPS and PBMC+ LPS+ DMF and PBMC+LPS+DMF+NIC when compared to the PBMC+vehicle group. Moreover, there was no statistical difference in the fluorescence intensity between PBMC+LPS+DMF group and PBMC+LPS+DMF-NIC group. LPS increases inflammation by enhancing the expression of TNF-α in the PBMC [156]. In previous studies, DMF and nicotinamide have been shown to possess anti-inflammatory activity by

suppressing the expression of TNF-α, analogy in the results can be seen in this study as well [177, 178].

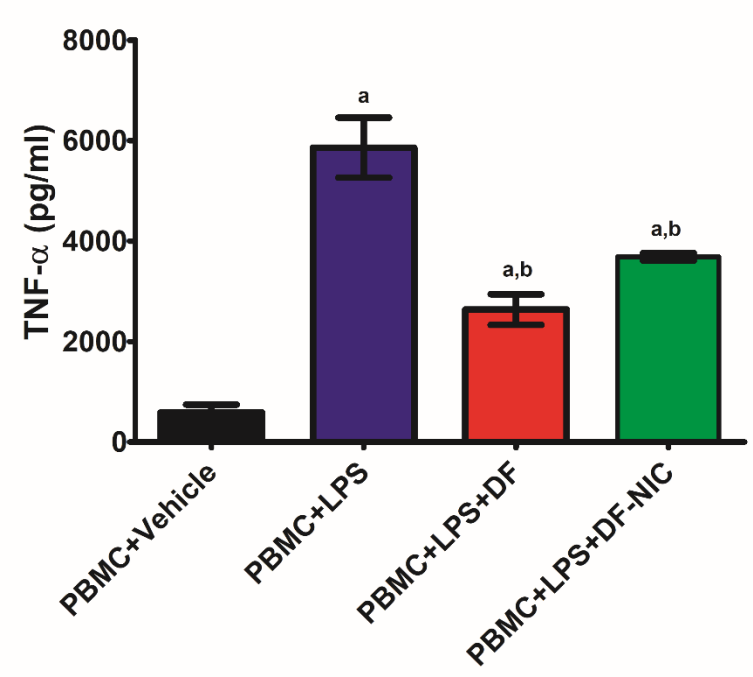

Figure 3-13 Showing TNF-α activity on treatment with DMF and DMF-NIC after LPS induction in PBMC.

All values are expressed as mean ± SEM (n=3). [a]p< 0.05 compared to PBMC+vehicle, [b]p< 0.05 compared to PBMC+LPS, [one-way ANOVA followed by Newman-Keuls Test].

3.5.14 Acute gastric acid model

With reference to the **Figure 3-14** shown below, statistical analysis using one-way ANOVA revealed a significant difference in ulcer area, [F (2, 9) = 38.27, p<0.05]. The post-hoc test revealed significant ulcerated areas in the DMF and DMF-NIC cocrystal treatment group when compared to the control group, Statistically, the DMF group has significantly more ulcerated areas when compared to DMF-NIC cocrystal. DMF has dose-dependently been shown to cause ulcers, mucosal damage and necrosis in rat and monkey models [67]. The ulcer protective effect of nicotinamide has been shown in previous studies as well [136].

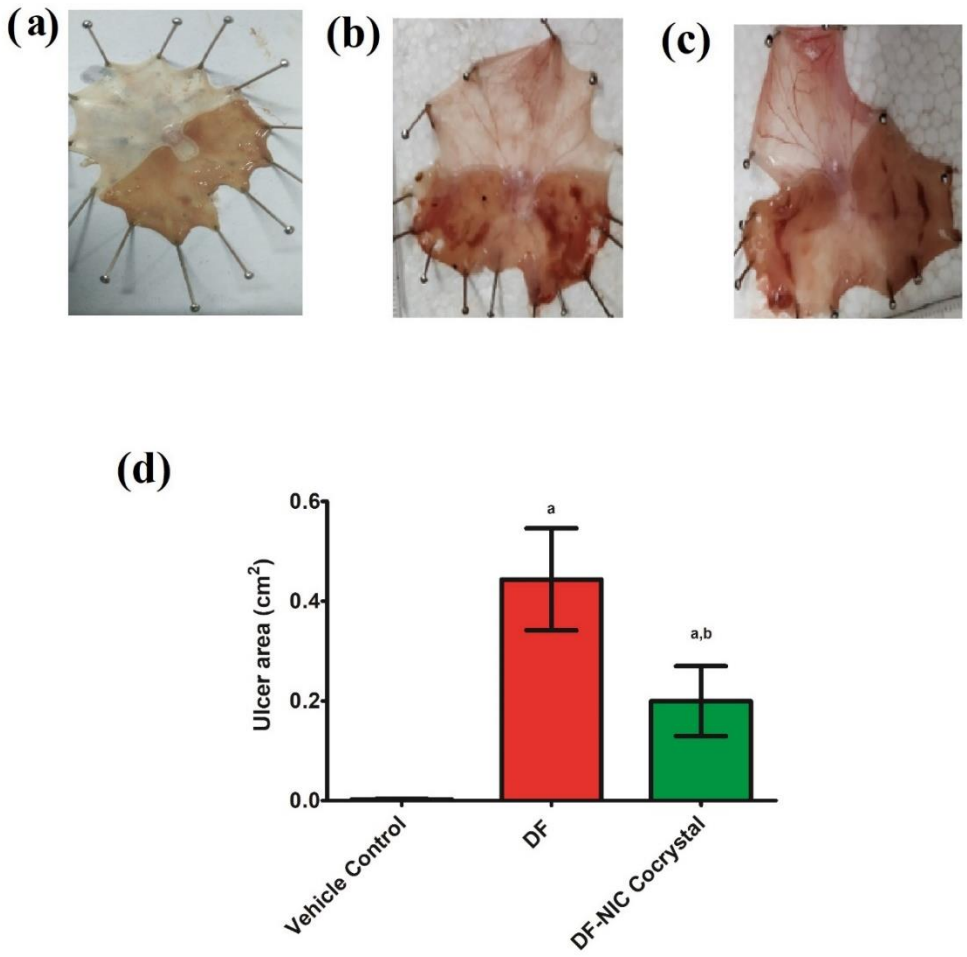

Figure 3-14 Showing ulcer area (cm^2) on treatment with DMF and DMF-NIC cocrystal.

All values are expressed as mean ± SEM (n=3). [a]p< 0.05 compared to Vehicle control, [b]p< 0.05 compared to DMF [one-way ANOVA followed by Newman-Keuls Test].

3.5.15 Acetic acid-induced gastric healing

With reference to the **Figure 3-15** shown below, statistical analysis using one-way ANOVA revealed significant differences in ulcer index, [F (4, 10) = 107.5, p<0.05] The post-hoc test revealed significant ulcer index in acetic acid+ vehicle treatment group, acetic acid+DMF, acetic acid+cimetidine and acetic acid+DMF-NIC Cocrystal treatment group when compared to the control group, Statistically, DMF group has significantly more ulcerated area when compared to DMF-NIC cocrystal. The DMF has an ulcerogenic effect as shown in the previous study [67] which can justify the high ulcer index in the

group and nicotinamide has a comparative gastroprotective activity which has imparted to low gastric index in the DMF-NIC cocrystal group [136].

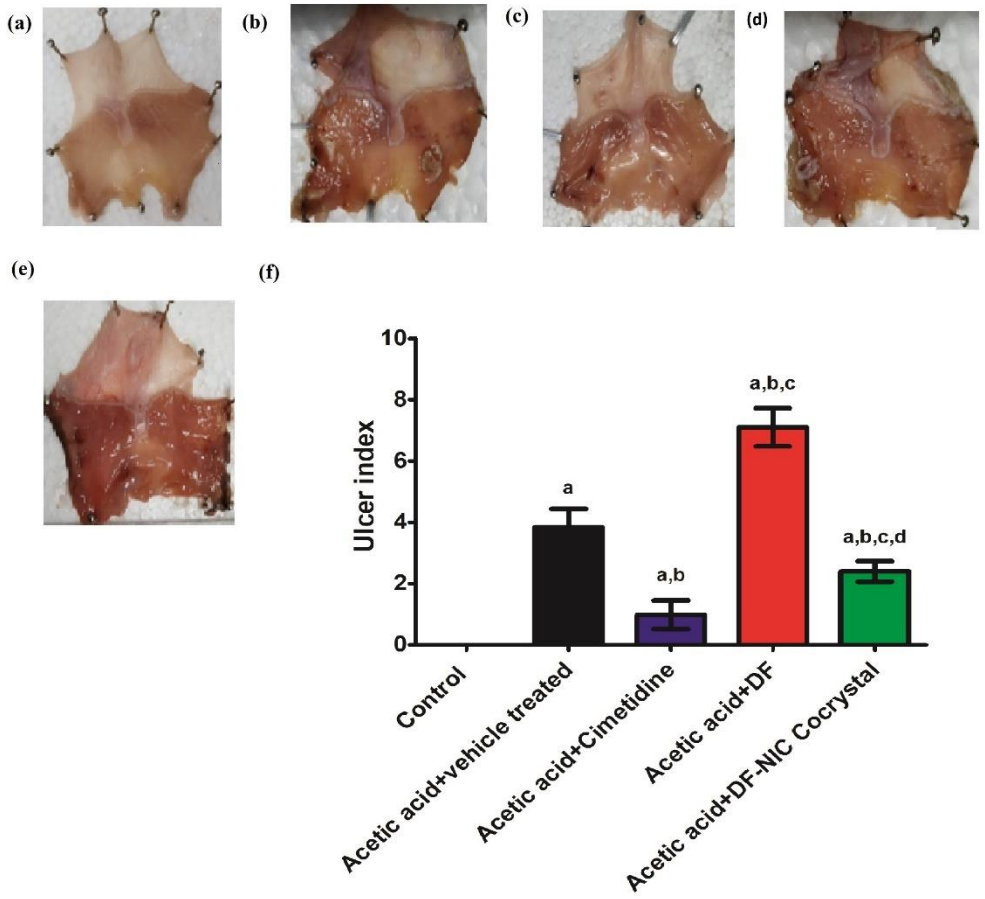

Figure 3-15 **Showing ulcer index on treatment with DMF and DMF-NIC cocrystal after acetic acid-induced ulcer.**

All values are expressed as mean ± SEM (n=3). [a]p< 0.05 compared to control, [b]p< 0.05 compared to acetic acid+ vehicle treated, [c]p< 0.05 compared to acetic acid+cimetidine, [d]p< 0.05 compared to acetic acid+ DMF [one-way ANOVA followed by Newman-Keuls Test].

3.5.16 Acetic acid-induced gastric healing by MDA activity

With reference to the **Figure 3-16** shown below, statistical analysis using one-way ANOVA revealed significant differences in lipid peroxidation, [F (4, 20) =28.86, p<0.05]

The post-hoc test revealed a significant increase in the lipid peroxidation in acetic acid+vehicle treatment group and acetic acid+DMF compared to the control group. However, there is no significant difference between the control, Acetic acid+DMF-NIC and acetic acid+cimetidine group. Moreover, the acetic acid+vehicle treatment group and acetic acid+DMF group have significantly more lipid peroxidation when compared to the DMF-NIC cocrystal and acetic acid+cimetidine group. Gastric ulcer is associated with elevated MDA levels due to reactive oxygen species which may in turn promote lipid peroxidation [179].

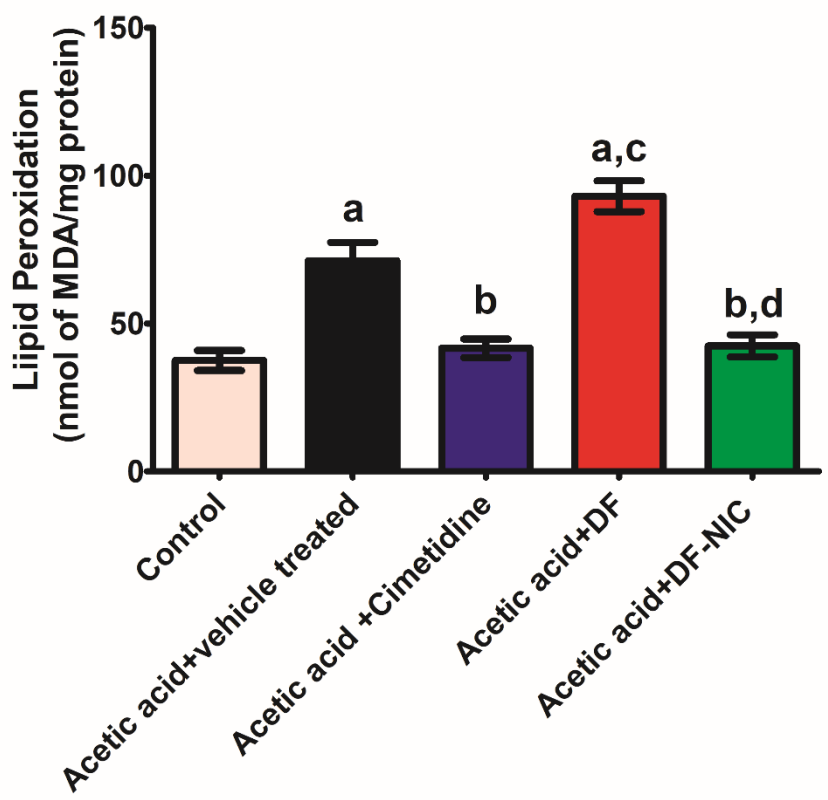

Figure 3-16 Showing lipid peroxidation in gastric tissue homogenated on treatment with DMF and DMF-NIC after acetic acid-induced ulcer.

All values are expressed as mean ± SEM (n=3). [a]p< 0.05 compared to control, [b]p< 0.05 compared to acetic acid+ vehicle treated, [c]p< 0.05 compared to acetic acid+cimetidine, [d]p< 0.05 compared to acetic acid+ DMF [one-way ANOVA followed by Newman-Keuls Test].

3.5.17 Total Nitrite level

Acetic acid-induced gastric healing: With reference to the **Figure 3-17** shown below, statistical analysis using one-way ANOVA revealed significant differences in total nitrite level, [F (4, 20) =26.09, $p<0.05$] The post-hoc test revealed a significant decrease in the total nitrite level in acetic acid+vehicle treatment group and acetic acid+DMF compared to the control group, Acetic acid+DMF-NIC group and acetic acid+cimetidine group. However, there is a significantly reduced nitrite in t-e Acetic acid+DMF as compared to the acetic acid+vehicle treated group. Gastric total nitrite and nitrate have gastroprotective effects [180] and their reduced levels are found in the acetic acid-induced gastric ulcer model [179]. DMF is known to cause gastrointestinal (GI) adverse effects [67]. Nicotinamide illicit gastroprotective effects [136] by increasing the nitric oxide which is attributed to the availability of an important cofactor called NADPH, crucially involved in the biogenesis of nitric oxide from arginine amino acid [181].

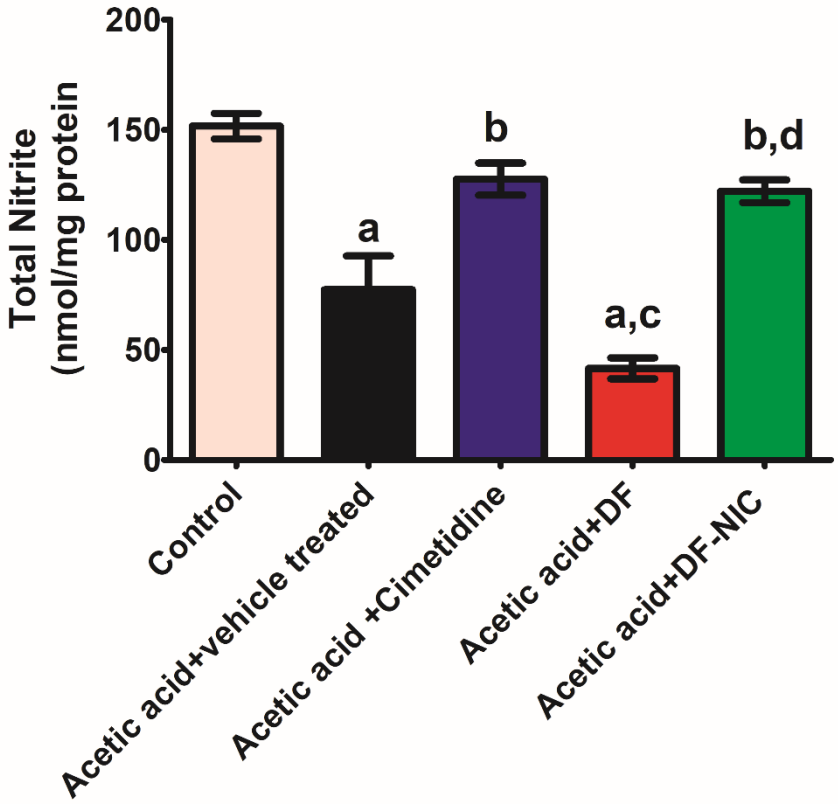

Figure 3-17 Total nitrite in gastric tissue homogenate on treatment with DMF and DMF-NIC cocrystal after acetic acid induced ulcer.

All values are expressed as mean ± SEM (n=3). [a]p< 0.05 compared to control, [b]p< 0.05 compared to acetic acid+ vehicle treated, [c]p< 0.05 compared to acetic acid+cimetidine, [d]p< 0.05 compared to acetic acid+ DMF [one-way ANOVA followed by Newman-Keuls Test].

3.6 Summary

Cocrystals of DMF with NIC as a coformer were done based on their predictability to participate in hydrogen bonding and GRAS (generally regarded as safe). Cocrystals have been formulated by using the solvent evaporation method and characterized by using spectral techniques of FTIR and diffractometry techniques of PXRD. The thermal evaluation has been done using TGA and DSC. Dissolution and pharmacokinetic studies compare the release profile of DMF with its cocrystal in in-vitro and in-vivo systems respectively. The cytotoxic and biological activity of DMF has been compared with that of the cocrystals. For the very first time, DMF cocrystals have been made to troubleshoot its sublimation problem and to counterbalance its adverse effects which will ultimately lead to enhanced processability of the API during its formulation and patient safety and compliance.